MEDICAL PHYSICS PUBLISHING

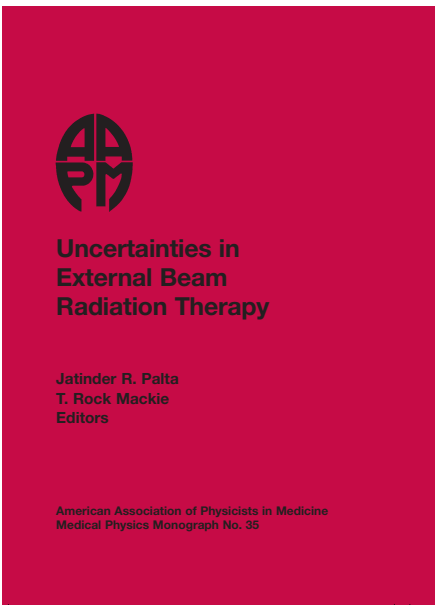

Here is a sample chapter from this book.

This sample chapter is copyrighted and made available for personal use only. No part of this chapter may be reproduced or distributed in any form or by any means without the prior written permission of Medical Physics Publishing.

Chapter 10

Limits of Precision and Accuracy of Radiation Delivery Systems

Jean M. Moran, Ph.D.[1] and Timothy Ritter, Ph.D.[2]
[1]Department of Radiation Oncology
University of Michigan, Ann Arbor, Michigan
[2]Ann Arbor Veterans' Affairs Hospital, Ann Arbor, Michigan

1 Introduction 215
2 Uncertainties in Beam Generation, Shaping, and Delivery 215
2.1 Spot Size 216
2.2 Beam Energy and Fluence 216
3 Uncertainties in Beam Shaping and Delivery 216
3.1 Monitor Chamber 218
3.2 In-Air Output Ratio (S_c) 218
3.3 Jaw Accuracy 218
3.4 Wedges 219
3.5 MLC Positioning Accuracy 219
3.5.1 Non-IMRT Delivery 219
3.5.2 IMRT Delivery 220
3.6 Treatment Couch 221
3.7 Tomotherapy 223
4 Protons 225
5 Delivery System Measurement Uncertainties 225
6 Summary 227
7 Future Considerations 228
References 228

1 Introduction

This chapter discusses sources of treatment delivery uncertainties that are independent of the patient. Components that are dependent upon the delivery technique are also discussed. These factors should be considered when determining the total uncertainty of dose to an individual patient. Uncertainties in beam calibration and in the modeling of machine parameters in the treatment planning system are deliberately excluded.

2 Uncertainties in Beam Generation, Shaping, and Delivery

The initial source of uncertainties is related to the generation of electron and photon beams for linear accelerator–based systems. Fundamental quantities of these accelerators such as the energy of the electrons incident on target, spectral width, beam divergence, and the resultant energy spectra are difficult to measure. Most of the

detailed measurements and analyses of these parameters have been performed as part of the development of improved Monte Carlo models of the full linear accelerator systems. The report of AAPM Task Group 105 (TG-105) provides an excellent detailed overview of clinical considerations for Monte Carlo algorithms for radiotherapy calculations (Chetty et al. 2007).

Monte Carlo methods have been used to verify information provided by the manufacturer as well as to assess the impact of individual beam model parameters on the resultant dose distribution (Sheikh-Bagheri and Rogers 2002; Chibani and Ma 2007). For example, when using measured depth dose curves or large field off-axis factors, Sheikh-Bagheri and Rogers were able to estimate the electron beam incident energy within 0.2 MeV using the BEAM Monte Carlo code (uncertainty at 0.7% at the 1 standard deviation (SD) level) (Sheikh-Bagheri and Rogers 2002).

2.1 Spot Size

Sawkey and Faddegon (2009a) investigated key parameters in the beam model by disassembling the treatment head components, performing measurements in three configurations to determine the parameters (beam energy, spectral width, spot size, and flattening filter densities), and then constraining the Monte Carlo model by these measured values. When simulating 6 and 18 MV x-ray beams, agreement between measurements and calculations deeper than the build-up region was wtihin 1.5%/1 mm. In the build-up region the agreement was 1.5%/1.5 mm at 6 MV and 2%/2 mm at 18 MV (Sawkey and Faddegon 2009b). The measured spot sizes were between 1.2 and 2.1 mm depending on energy and direction, with in-plane spot sizes considerably smaller than cross plane dimensions. Sonke et al. (2003) demonstrated that the focal spot of a linear accelerator is not stationary and moves up to 0.7 mm at the start of irradiation.

2.2 Beam Energy and Fluence

The beam energy and fluence have primarily been investigated using Monte Carlo methods. For example, Rogers et al. (1995) benchmarked the BEAM code for different electron beams by comparing simulations and measurements. They also used the BEAM code to study the energy spectra for electron beams in more detail. Ding et al. (1996) investigated the electron mean energy for clinical electron beams as a function of depth using the BEAM code to simulate the full treatment head. They found differences in the depth-scaling factors as a function of the material for different types of plastic compared to water.

3 Uncertainties in Beam Shaping and Delivery

There are a number of uncertainties in beam delivery that affect the dose in the central region and penumbra. Table 10–1 presents an estimate of the uncertainties

Table 10–1. A Summary of the Estimated Uncertainty and Ability To Measure for Components of a Linear Accelerator

Component	Reference Examples	Estimated Uncertainty	Notes with Respect to Measurements	Dosimetric Impact
S_c	Zhu et al. 2009, Weber et al. 1997	0.5%–1%	Straightforward with correct equipment (S_c phantom, chamber, build-up caps)	Impact: minimal for large fields; larger for small fields
Jaw positioning accuracy	Kutcher et al. 1994 Rosenthal et al. 1998 Klein et al. 2009	<1 mm	Typically measured with graph paper, high resolution dosimetry to be used when assessing abutted fields	Impact: minimal impact on output for large fields; greater than 15% dose uncertainty for abutted fields with 1 mm gap or overlap
Wedges	Klein et al. 2009	2%/2 mm	Estimated using TG-142 tolerances (monthly and annual tests)	Depends on depth, wedge angle, and distance off axis
MLC position – static	Huq et al. 2002 Abdel-Hakim et al. 2003)	≤1 mm, leaf end/edge transmission highly variable	Straightforward relative check with picket fence test	Minimal impact with sufficient margins. Caution with field edge matching using MLCs (up to 20% discrepancy at match edge) and small field sizes/beamlets
MLC dynamic	LoSasso et al. 1998	Typically ≤1 mm	Measure output for narrow "sliding window"	Dose discrepancy highly dependent on gap between adjacent leaves
MLC transmission	Ezzell et al. 2009	Up to several percent with highly modulated IMRT fields	Discriminate between interleaf and intraleaf leakage or measure average value	Does not vary (but lack of modeling 1.5%–3% for static fields)

(continued)

Table 10–1 *(continued).* A Summary of the Estimated Uncertainty and Ability To Measure for Components of a Linear Accelerator

Component	Reference Examples	Estimated Uncertainty	Notes with Respect to Measurements	Dosimetric Impact
Tabletop (or couch)	McCormack et al. 2005 and others (see text)	Depends on angle, energy, and position. Attenuation up to 20% for extreme conditions	Can measure with ion chambers, EPIDs, and other methods	Beam attenuation: up to 13% for couch top; 15% for support rails. Can spoil skin sparing

for different components along with notes regarding the measurements of uncertainty and the dosimetric impact. References in the literature are listed for each value with additional detail provided in the text.

3.1 Monitor Chamber

Backscatter into the monitor chambers has been measured (Lam et al. 1998) and also shown with Monte Carlo to have a 2% to 3% effect on output for a range of field sizes and energies for photon and electron beams (Liu et al. 2000; Verhaegen et al. 2000).

3.2 In-Air Output Ratio (S_c)

The in-air output factor, or collimator scatter factor (S_c), varies with field size for photon beams. AAPM TG-74 report presents a theoretical derivation for S_c and an approach for reliably measuring it, including for small fields (Zhu et al. 2009). Values of S_c are very similar for a given type of accelerator but can vary by manufacturer and model. The report also includes a table of S_c values by manufacturer and model with a measurement uncertainty of 0.5% for square and rectangular open fields. Accurate determination of S_c depends upon using the proper equipment for measurement and appropriate correction factors (when necessary). For example, Weber et al. (1997) showed deviations up to 1% in S_c values as a function of field size for 18 MV depending on whether a lead or a brass build-up cap was used for the measurements.

3.3 Jaw Accuracy

The jaw setting affects the fluence, scatter, and the determination of the beam edge. The jaw setting also affects the monitor chamber reading due to backscatter of elec-

trons and photons from the collimators. For large fields, variations of 1 mm typically have a minimal impact on the central dose region. When fields are abutted or matched at the jaw edges, small deviations in position may result in large local dose differences. Abutted fields were at one time commonplace in head and neck treatments and still find frequent use in the clinic. The dose discrepancy at a match line is demonstrated as a thin line of either under or over dosing with a magnitude that is dependent on the energy, penumbra, and depth (among other factors). Several authors have published investigations into this phenomenon. Saw and Hussey (2000) reported that edge mismatches of ±1 mm and ±2 mm result in dose non–uniformities of 17% and 35%, respectively, with measurements taken at a depth of dose maximum for a 6 MV beam. Rosenthal et al. (1998) report similar results for a range of energies, concluding that a 2-mm gap or overlap can produce a match line dose that deviates 30% to 40% from the desired values.

3.4 Wedges

The estimated uncertainty for wedges is approximately 2%/2 mm. The AAPM TG-142 report defines tolerance values (Kutcher et al. 1994; Klein et al 2009). The effect of the uncertainty depends on the depth and energy, with increased variation expected as wedge angle and off-axis distance along the heel-toe direction increase.

3.5 MLC Positioning Accuracy

Multileaf collimators (MLCs) are widely used for beam shaping, beam blocking, and intensity modulation. Current MLC systems use tungsten leaves with either divergent or nondivergent leaf edges. The leaf edges and sides, leaf width, leaf thickness, and use of a backup collimator are important considerations that impact delivered dose. The distance from the target to the leaves varies with manufacturer and affects penumbra width as well as skin dose and backscatter into the monitor chamber (Huq et al. 2002). Ideally, for error free dose delivery and targeting, the MLC must be centered along the collimator axis of rotation, aligned perfectly to the jaws (if the MLC is backed up by jaws), capable of driving each leaf to the exact desired leaf position with zero error, and able to achieve leaf speeds instantaneously and reproducibly at all gantry angles during delivery. In reality, the expected leaf imprecision for static fields is typically 1 mm or less and minimally impacts the dose for large apertures. A more concerning match line discrepancy can result when MLC leaf edges are matched to jaws or to other MLC edges, or when tongue and groove effects come into play during intensity-modulated radiation therapy (IMRT) treatments. In addition, when IMRT fields are delivered with small static segments or dynamic delivery, any deviation in leaf edge placement can lead to a dose error.

3.5.1 Non-IMRT Delivery

The interleaf and intraleaf MLC leakage impact the dose delivered to the planning target volume (PTV). The error introduced by the intra- and interleaf leakage

depends on how accurately the MLC is represented in the planning system. Many planning systems do not separately address interleaf leakage and interleaf leakage, instead relying on an average value for both. Interleaf leakage, also called "leaf transmission," results in small (1 mm or less wide) strips of slightly increased dose at the spatial frequency of the MLC leaf spacing. The peak-trough amplitude is typically less than 1% of the delivered dose (Huq et al. 2002). The magnitude of this leakage depends highly on whether backup collimators also attenuate the delivered radiation.

A noticeable dose discrepancy may result if MLCs are used at a match line between adjacent fields. Abdel-Hakim et al. (2003) investigated this problem for four different match situations (side-side, side-end, end-side, and end-end) and reported dose discrepancies of up 20%. Fortunately the leaf ends could be adjusted to result in nearly homogenous doses for all cases except the side-side match, where an underdose of 15% was observed. This underdose, attributed to the tongue-and-groove effect, was also investigated by Huq et al (2002), who reported that tongue-and-groove effects at 6 MV reduced the dose at the match line by 14% to 33%, depending on the MLC design.

3.5.2 IMRT Delivery

The tongue-and-groove effect may come into play during IMRT delivery using both the segmental and dynamic delivery modes. In these cases, the magnitude of the effect depends on the energy, leaf sequencing, number of beams, and depth in the patient, among other parameters. The tongue-and-groove effect is very narrow in dimension, with a full-width half maximum (FWHM) of 2.5 mm or less (Losasso 2003). Deng et al. (2001) reported that for a single 15 MV IMRT field, this effect could cause an underdose of almost 10%. But the typical multi-field plan dilutes the impact of tongue and groove; and when the other treatment fields were considered, the dose deviation in the target dropped to only 1.6%. The addition of patient position uncertainties further reduced the dose discrepancy.

One of the most significant sources of delivery uncertainty associated with the MLC is the gap between opposing leaves. As this gap between the leaves becomes smaller, the accuracy and precision of the leaf positions becomes critical if the proper dose is to be deposited. LoSasso et al. (1998) determined the relationship between the nominal desired gap and the dose error as a function of different gap errors for a dynamically delivered IMRT plan. For example, they showed that a 0.5 mm gap error can result in a 5% dose error if the desired leaf gap is nominally 1 cm. Sharpe and colleagues also investigated this effect for small field sizes and reported that a 1 mm deviation in field size resulted in a nearly 8% dose discrepancy for a 1×1 cm^2 18 MV field (Sharpe et al. 2000). Dynamic delivery has the added complication that the beam remains on during treatment delivery. Deviations in leaf speed can therefore lead to gap errors and should be monitored. It is important to understand that these deviations represent a worst-case scenario assuming all dose is deposited using the single maladjusted field.

Another potential source of inaccuracy for IMRT delivery is the inability to deliver a small number of monitor units (MUs) repeatedly and accurately. The accuracy of the delivery is limited by the communication between the MLC control system and the linac controller (Ezzell and Chungbin 2001; Litzenberg et al. 2002). A general level of dosimetric uncertainty is difficult to predict since the total delivered MUs, the sequencing of each individual field, and the dose delivery rate impact the end result. Ezzell and Chungbin (2001) showed that for standard treatment plans and dose rates (400 MU/min) the maximum error in delivered MUs for one manufacturer's control system was ±0.6 MUs. While this can affect many fields the overall clinical impact is minimal (Ezzell and Chungbin 2001). Palta et al. (2003) investigated the dose rate dependence of this effect and reported that small segments can be completely missed during delivery at high dose rates.

It is clear that the MLC and the delivery system interact in a complex manner during the delivery of IMRT. Palta et al. (2003) created a comprehensive table of tolerance and action limits for IMRT treatment delivery. They considered the relevant variables and recommended tolerance limits to maintain the dose to within 3% of the desired value. Action limits were set at twice the tolerance limits.

With respect to arc therapy delivery, several of the leaf reproducibility tests developed for static IMRT delivery have been modified for use in volumetric arc therapy delivery (Ling et al. 2008). Bedford found one system to be reproducible with delivery at different dose rates and modulation (Bedford and Warrington 2009). As these systems are installed in more centers, it is expected that measured data will be gathered on the different delivery uncertainties such as gantry rotation speed, beam modulation, and MLC factors such as leaf speed.

3.6 Treatment Couch

Attenuation by the treatment couch is a factor that has traditionally been neglected in treatment planning. Recently a number of investigators have evaluated the impact of the couch top on the delivered dose. Because of the variability in the amount of attenuation, this section presents a more detailed evaluation of the literature.

High-energy photon beams are typically delivered from a variety of treatment angles in either coplanar or non-coplanar arrangements. Some treatment angles, especially ones delivered from the posterior of the patient, may pass through sections of the patient support system to include the couch top and the supporting framework. Modern patient support systems are often fabricated from carbon fiber materials with minimal attenuation; however, these systems can still attenuate the beam significantly and degrade the skin sparing effect. In some cases, the impact on the dose distribution can be effectively modeled in the planning system. In other cases, such as when supporting struts under the table may intersect the beam, the setup cannot be easily modeled and the beam arrangement for patient treatment may need to be changed.

The attenuation of the patient support (or couch) depends significantly on the specific couch design, the gantry angle, the beam energy, the field size, and in many cases the position of the patient on the table. Reported attenuation factors for the couch surface alone vary from less than 2% to as high as 13.3% (McCormack et al. 2005; Munjal et al. 2006; Poppe et al. 2007; Mihaylov et al. 2008; Li et al. 2009; Njeh et al. 2009; Gerig et al. 2010; Hayashi et al. 2010; Smith et al. 2010). A traditional tabletop surface with a "tennis racket" insert may demonstrate negligible attenuation for a high-energy beam at normal incidence; however, support systems designed specifically for image guidance (that minimize imaging artifacts) incorporate a uniform density and may have significant attenuation. Njeh reported attenuation of up to 10% (at 6 MV) and 3.6% (at 18 MV) for one design (Njeh et al. 2009); Marguet measured attenuation values of up to 4.1% (at 6 MV) and 2.2% (at 18 MV) for a second system (Marguet et al. 2010); and a third system demonstrated an attenuation of 4.6% at 6 MV (Spezi and Ferri 2007). Besides the couch itself, table extensions used for treatment of the head and neck as well as head supports deserve consideration. Headrest attenuation of up to 6.3% was measured by Njeh at 6 MV. Gajdos assessed the attenuation properties of three different extension designs and reported a peak value greater than 13% (Gajdos et al 2005). Since the reported values for attenuation vary over such a wide range, physicists must evaluate the attenuation properties of their patient support surface and use the information appropriately.

In addition to the attenuation provided by the treatment couch surface, the structure supporting the couch or securing the immobilization apparatus may intercept the beam and reduce the dose delivered to the patient. For example, one design uses sliding rails that can be moved out of the path of the treatment beam. Li et al. (2009) discussed an attenuation of up to 26.8% for 6 MV photon beams when the sliding rails and the couch surface were in the beam path, while the attenuation for just the couch surface was measured at 13.3%. Vieira et al. (2003) used an electronic portal imaging device to measure the attenuation for typical patient setups. They found that for head and neck immobilization, the couch rails could attenuate a 6 MV beam by 15% at an unfavorable gantry angle. The attenuation by other components of the patient support system was also measured. For example, the pin use to attach the mask was found to have an attenuation of 10% (Vieira et al. 2003).

The couch can alter not only the absolute dose but also the relative dose distribution in the patient. This is particularly true in the first centimeter of patient tissue proximal to the couch. A medium adjacent to the skin may act as "build-up" and increase the surface dose, reducing the skin sparing benefit of high-energy photon beams. Gerig et al. (2010) report a worst-case scenario where the surface dose was increased from 17% to 88% by a high-energy photon beam passing through one model of a carbon fiber couch. Similar results were reported by Poppe et al. (2007), who found surface doses up to 120% of the dose measured at 5 cm depth, indicating that the skin sparing effect was almost completely negated for 6 MV and 10 MV beams. Energy, gantry angle, field size, and beam modifiers are all important variables when evaluating the loss of skin sparing. Smith et al. (2010) investigated

another couch design and found that again nearly all skin sparing was lost when the angle of incidence on the couch was oblique. Other authors report similar results and confirm the need to consider the build-up effect of the treatment couch (Higgins et al. 2001; Spezi and Ferri 2007; Benhabib et al. 2010; Court et al. 2010).

It is possible to quantify and account for the effects of the patient support system during the treatment planning process. Gerig et al. (2010) describes results for two different couch tops modeled in a commercial treatment planning system. They showed that modeling of the couch top led to an error of less than 2% between calculated and measured results as a function of gantry angle for a 10×10 field. It is important to consider that accurate prediction of surface dose is problematic for all but the most sophisticated algorithms, and this is independent of whether the couch is present or not. The steep nature of the build-up curve at the skin surface can actually point to more accurate surface dose predictions with the couch in place, the couch serving to move the skin dose to a less steep region of the build-up curve. Other studies have demonstrated errors of approximately 2% or less at depth for other combinations of advanced treatment planning systems and couches (Myint et al. 2006; Mihaylov et al. 2008; Van Prooijen et al. 2010), with Smith adding a note of caution regarding specific pencil beam and convolution-only algorithms (Smith et al. 2010).

The final and most important concern when discussing the impact of the patient support system is the impact on PTV coverage. Only a fraction of the beams are typically delivered from gantry angles that intersect the couch, and only a subset of those gantry angles may pose problems. Van Prooijen performed a retrospective study on plans that presented potential intersections of the beam and the couch and reported compromised PTV coverage by up to 3% and slightly reduced (1%) CTV coverage (Van Prooijen et al. 2010). Li presented a 9-field IMRT case with two posterior beams that could be potentially delivered through the couch rails, resulting in a dose reduction of 2.5% (Li et al 2009). It is easy to conceive scenarios where the dose delivered to the PTV would be reduced by more than 3%, especially when lower-energy photon beams are used to treat posteriorly located lesions. For those cases extra caution is warranted.

3.7 Tomotherapy

Helical tomotherapy treatment delivery differs significantly compared to conventional linear accelerator therapy and deserves special consideration. All delivered therapies on a Hi-Art® tomotherapy unit (TomoTherapy Inc., Madison, WI) are dynamic IMRT treatments involving simultaneous gantry, MLC, and couch movement. The output is determined as a function of dose per unit time rather than dose per monitor unit. The two monitor chambers in the treatment head are used solely to turn off the beam if the measured dose rate deviates substantially from the nominally expected value. Dose rate deviations of up to 50% from the nominal value can be tolerated for very short periods before the beam is shut off. The dosimetric impact of this magnitude of dose rate fluctuation is unknown (Langen et al. 2010).

Helical tomotherapy machines are calibrated using a static gantry geometry, a setup which is not used to deliver any patient treatments. A second reference measurement is then performed using a dynamic delivery method that mimics the way patients are treated. MLC motion is binary, with leaf positions being either closed or open. The pitch, defined as the couch travel in one gantry rotation divided by the treated slice width, plays an important role in dose delivery. The pitch selected during the planning process impacts leaf opening times, which in turn impacts actual delivered dose (Westerly 2009). In addition, the cyclic nature of helical delivery interacts with beam divergence to result in the "thread" effect (Langen et al. 2010). Pitches of 0.86/n (where n is an integer) should be used during planning to minimize the thread effect when possible. If other pitches are used then the deviation in delivered dose, which can be on the order of several percent for off-axis points treated at larger pitch values, should be assessed (Kissick et al. 2005). Planning, calibration, delivery method, quality assurance, and uncertainty for a TomoTherapy unit are therefore all unique.

Broggi et al. (2008) reported the results of a 2-year study on helical tomotherapy quality assurance in 2008 in which 496 static output measurements demonstrated an average variation of –0.1% but a standard deviation of 1.0%. Similar results were reported by the same author for rotational output checks, with the resultant interpretation that output for the particular tomotherapy unit measured may be "slightly inferior compared with a conventional linac." Energy constancy, defined as a ratio of the dose at 20 cm and 10 cm depths, demonstrated an average error of –0.4% with an SD of ±0.4%. Many of the mechanical parameters such as jaws, MLC position, and MLC-detector array-gantry rotation plane alignment were found to display excellent stability with deviations less than 1 mm. The gantry-couch synchronization, a crucial element in helical delivery, showed an average disagreement of 1.3 mm ±0.6 mm when assessed over a 30-cm travel distance. Profile constancy was found to fall within the range –0.9% to +0.8%.

Other investigators have reported results similar to those of Broggi et al for helical tomotherapy machine performance tests (Fenwick et al. 2004; Mahan et al. 2004; Thomas et al. 2005). The day-to-day output consistency findings of Van Esch et al. (2007) confirm Broggi's findings that the output stability of helical tomotherapy lies somewhere in the range of 1% to 2%. Out-of-field dose has been addressed by Ramsey et al. (2006) who showed that even with the long beam-on times associated with the TomoTherapy system, the peripheral doses are comparable to, and possibly lower than, the values reported for treatments on conventional linacs.

Because of the non-intuitive and complex nature of helical tomotherapy delivery, it is difficult to assess uncertainty in overall dose delivery. The numerous studies comparing planned to delivered doses do not tease out the sources of the disagreement between the two. It is possible that repeated measurements on the same dynamic treatment plan can shed some light on the problem. Broggi performed a daily test of IMRT delivery using two ion chamber measurements over a period of 2 years. Dose deviations of –0.5%±1.2% for a low-dose gradient point

and –0.4%±2.2% for a high-dose gradient point were reported (Broggi et al. 2008). The influence of measurement uncertainty on these results cannot be determined but is likely significant for the high-dose gradient point. The low-dose gradient SD of 1.2% points to a day-to-day dose variation of ±2.4 % at a 95% confidence interval.

4 Protons

Several of the uncertainties described here can lead to greater uncertainty in proton therapy. For example, attenuation by different thicknesses of a tabletop would have a greater impact on the range of protons. Techniques and detectors are under development to better understand the uncertainties. Moyers et al. (2007) reported on the calibration of a monitor for beam energy, a result of the need to know the absolute proton energy to within 1 MeV. This calibration technique was validated for proton energies of 40 to 255 MeV. With respect to a proton gantry, Ciangaru et al. (2007) modified a traditional Winston-Lutz test to verify the coincidence of a proton beam with the gantry mechanical isocenter. They found the deviation between the proton beam central axis and the gantry mechanical isocenter to be 0.22 mm, with a ±0.1 mm uncertainty for their film-based technique. Further developments are expected in this area.

5 Delivery System Measurement Uncertainties

There are measurement uncertainties related to the delivery system as well as those related to the measurements themselves. A detailed investigation of the types of measurement uncertainties has been conducted by the Joint Committee for Guides in Metrology (JCGM 2008). The classes of evaluation of uncertainties are type A, where the uncertainty is evaluated by a statistical analysis of the data and type B, where the uncertainty is evaluated by non-statistical methods (JCGM 2008). Mitch et al. (2009) have compiled a detailed review of Type A and Type B for dosimeters in radiation therapy. The uncertainty of rulers and graph paper is 0.5 mm for a ruler in centimeter increments. Finer resolution measurements have been performed using film with a spatial resolution of approximately 0.1 mm.

With respect to dosimetric equipment, AAPM TG-106 (Das et al. 2008) on beam data commissioning and TG-120 on dosimetry for IMRT (Low et al. 2011) are examples of reports detailing the use of the correct dosimeters for different tasks. The applications of different detectors are discussed along with the advantages and disadvantages of each. For example, the response of ionization chambers is very reproducible, and they are excellent for measuring the output of photon beams greater than 5×5 cm^2. However, use of an ion chamber for penumbra measurements can lead to an inaccurate measurement as shown in Figure 10–1a, where an ion chamber measurement is compared to a diode for a profile measurement at depth for a 6 MV beam. The difference between the two detectors, shown in Figure 10–1b, is as high as 15% in the gradient region. Figure 10–2 shows a comparison of film

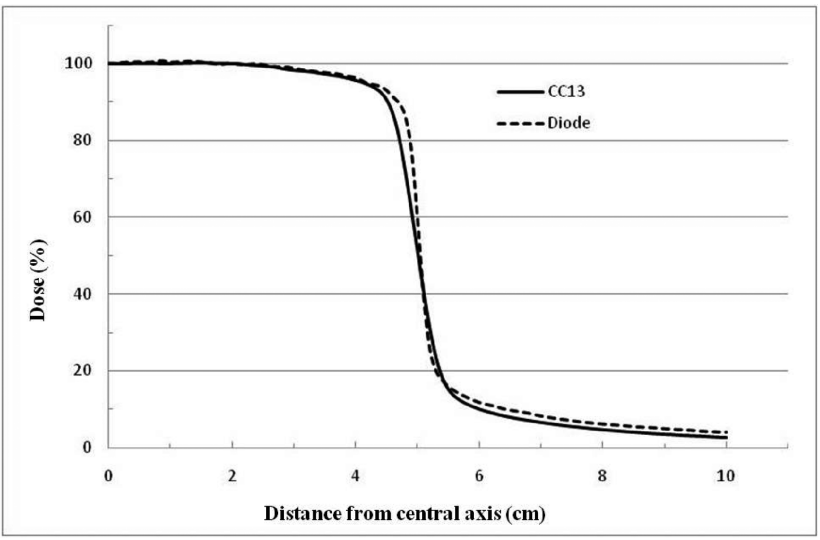

(a)

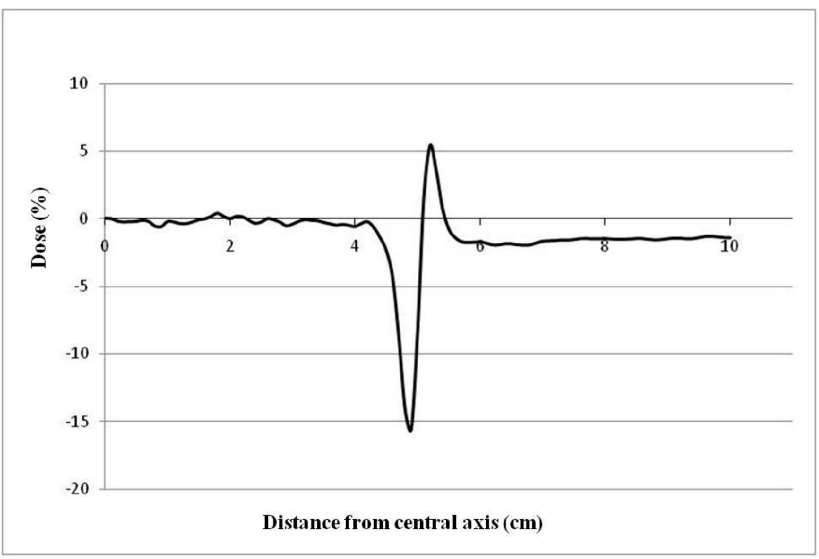

(b)

Figure 10–1. (a) Example of a profile (shown from central axis to one field edge) measured with an ion chamber (CC13) and a diode at 10 cm depth for a 6 MV 10×10 cm field (90 cm SSD). (b) Dose difference (in %) between the ion chamber and diode data shown in (a).

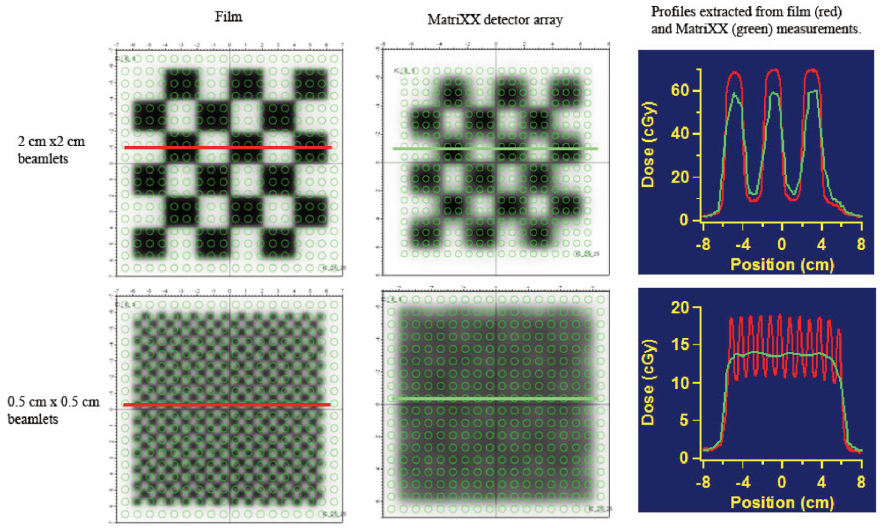

Figure 10–2. IMRT example demonstrating volume averaging for a 2D detector array compared to radiographic film. The measurements are shown with an overlay of the detector positions. An example of the profile is extracted from the film and detector array measurements to show the degradation of the detected signal (or blurring) due to the size of each chamber compared to the high spatial resolution film measurement).

to a two-dimensional (2D) ion chamber array (MatriXX, IBA Dosimetry, Germany) for checkerboard fields of alternating high and low intensity at two different beamlet sizes. The detector response is affected by volume averaging with the ionization chamber array compared to the high-resolution film measurements. Devices used for daily QA output measurements will have some uncertainty associated with the measurements. This is expected and tolerances for the use of these devices are set accordingly.

6 Summary

Many of the uncertainties in external beam therapy are well understood, with additional data being gathered for newer delivery techniques. Some factors are difficult to measure. In these areas, Monte Carlo techniques have been invaluable for investigating the sensitivity of the resulting distribution on parameters such as the spot size or incident electron energy. A number of sources of dose delivery uncertainty have been discussed and were summarized in Table 10–1. Many of these factors are

significant only when they are not modeled correctly, or accounted for, by the treatment planning system. Accurate commissioning, detailed validation, and understanding the limitations of the treatment planning system are therefore key steps in minimizing delivery uncertainties.

7 Future Considerations

The AAPM TG-100 is creating a report on the use of risk management tools such as Failure Modes and Effect Analysis (FMEA) for radiation therapy (Huq et al. 2012a,b). Other groups have begun to use such tools to revisit how the uncertainty and expected mode of failure impact their quality assurance processes. For example, Pawlicki et al. (2005) have used statistical process control to distinguish between systematic and random errors in output and flatness and symmetry. By tracking and analyzing the data consistently, it is possible to identify systematic changes. This information can be used to guide policies and procedures. Sawant et al. (2010) have performed an FMEA analysis for dynamic MLC tumor tracking systems. With the dramatic changes in the complexity of radiation therapy and the associated hardware and software systems, it is expected that our traditional models of quality assurance will continue to be revised as we learn more about utilizing engineering principles in guiding our practice.

References

Abdel-Hakim, K., T. Nishimura, M. Takaih, S. Suzuki, and H. Sakahara. (2003). "Dosimetric assessment of the field abutment region in head and neck treatments using a multileaf collimator." *Strahlenther Onkol* 179(5):312–319.

Bedford, J. L., and A. P. Warrington. (2009). "Commissioning of volumetric modulated arc therapy (VMAT)." *Int J Radiat Oncol Biol Phys* 73(2):537–545.

Benhabib, S., J. Syh, C. Austerlitz, M. Ferreira, and C. Sibata. (2010). "Investigation of Different Carbon Fiber Tabletops Used in Radiation Therapy." *Med Phys* 37:3328. [Abstract SU-GG-T-611]. 52nd AAPM Annual Meeting, July 18–22, 2010, Philadelphia, PA.

Broggi, S., G. M. Cattaneo, S. Molinelli, E. Maggiulli, A. Del Vecchio, B. Longobardi, L. Perna, F. Fazio, and R. Calandrino (2008). "Results of a two-year quality control program for a helical tomotherapy unit." *Radiother Oncol* 86(2):231–241.

Chetty, I. J., B. Curran, J. E. Cygler, J. J. DeMarco, G. Ezzell, B. A. Faddegon, I. Kawrakow, P. J. Keall, H. Liu, C. M. Ma, D. W. Rogers, J. Seuntjens, D. Sheikh-Bagheri, and J. V. Siebers. (2007). "Report of the AAPM Task Group No. 105: Issues associated with clinical implementation of Monte Carlo-based photon and electron external beam treatment planning." *Med Phys* 34(12):4818–4853. http://www.aapm.org/pubs/reports/RPT_105.pdf.

Chibani, O., and C. M. Ma. (2007). "On the discrepancies between Monte Carlo dose calculations and measurements for the 18 MV Varian photon beam." *Med Phys* 34(4):1206–1216.

Ciangaru, G., J. N. Yang, P. J. Oliver, M. Bues, M. Zhu, F. Nakagawa, H. Chiba, S. Nakamura, H. Yoshino, M. Umezawa, and A. R. Smith. (2007). "Verification procedure for isocentric alignment of proton beams." *J Appl Clin Med Phys* 8(4):2671.

Court, L., J. Urribarri, and M. Makrigiorgos. (2010). "Carbon fiber couches and skin sparing." *J Appl Clin Med Phys* 11(2):3241.

Das, I. J., C. W. Cheng, R. J. Watts, A. Ahnesjo, J. Gibbons, X. A. Li, J. Lowenstein, R. K. Mitra, W. E. Simon, and T. C. Zhu. (2008). "Accelerator beam data commissioning equipment and procedures: Report of the TG-106 of the Therapy Physics Committee of the AAPM." *Med Phys* 35(9):4186–4215. http://www.aapm.org/pubs/reports/RPT_106.pdf.

Deng, J., T. Pawlicki, Y. Chen, J. Li, S. B. Jiang, and C. M. Ma. (2001). "The MLC tongue-and-groove effect on IMRT dose distributions." *Phys Med Biol* 46(4):1039–1060.

Ding, G. X., D. W. O. Rogers, and T. R. Mackie. (1996). "Mean energy, energy-range relationships and depth-scaling factors for clinical electron beams." *Med Phys* 23(3): 361–376.

Ezzell, G. A., and S. Chungbin. (2001). "The overshoot phenomenon in step-and-shoot IMRT delivery." *J Appl Clin Med Phys* 2(3):138–148.

Ezzell, G. A., J. W. Burmeister, N. Dogan, T. J. LoSasso, J. G. Mechalakos, D. Mihailidis, A. Molineu, J. R. Palta, C. R. Ramsey, B. J. Salter, J. Shi, P. Xia, N. J. Yue, and Y. Xiao. (2009). "IMRT commissioning: Multiple institution planning and dosimetry comparisons, a report from AAPM Task Group 119." *Med Phys* 36(11):5359–5373. http://www.aapm.org/pubs/reports/RPT_119.pdf.

Fenwick, J. D., W. A. Tomé, H. A. Jaradat, S. K. Hui, J. A. James, J. P. Balog, C. N. DeSouza, D. B. Lucas, G. H. Olivera, T. R. Mackie, and B. R. Paliwal. (2004). "Quality assurance of a helical tomotherapy machine." *Phys Med Biol* 49(13):2933–2953.

Gajdos, S., L. Muhieddine, G. Chan, and M. Weinhous. (2005). "A Dosimetric Comparison of Three Commercially Available Carbon Fiber Table Extension Boards." *Med Phys* 32:1. [Abstract SU-FF-T-60}. 47th AAPM Annual Meeting, Seattle, WA, July 24–28, 2005.

Gerig, L. H., M. Niedbala, and B. J. Nyiri. (2010). "Dose perturbations by two carbon fiber treatment couches and the ability of a commercial treatment planning system to predict these effects." *Med Phys* 37(1):322–328.

Hayashi, N., Y. Shibamoto, Y. Obata, T. Kimura, H. Nakazawa, M. Hagiwara, C. I. Hashizume, Y. Mori, and T. Kobayashi. (2010). "Megavoltage photon beam attenuation by carbon fiber couch tops and its prediction using correction factors." *J Radiat Res* (*Tokyo*) 51(4):455–463.

Higgins, D. M., P. Whitehurst, and A. M. Morgan. (2001). "The effect of carbon fiber couch inserts on surface dose with beam size variation." *Med Dosim* 26(3):251–254.

Huq, M. S., I. J. Das, T. Steinberg, and J. M. Galvin. (2002). "A dosimetric comparison of various multileaf collimators." *Phys Med Biol* 47(12):N159–N170.

Huq, M. S., B. A. Fraass, P. B. Dunscombe, J. P. Gibbons Jr., G. S. Ibbott, A. J. Mundt, S. Mutic, J. R. Palta, F. Rath, B. R. Thomadsen, J. F. Williamson, and E. D. Yorke. TG-100 Report Part 1: Using Risk Analysis To Design Radiation Therapy Quality Management Programs: IMRT as a Case Study. Medical Physics Report No. (unassigned), To be published 2012a.

Huq, M. S., B. A. Fraass, P. B. Dunscombe, J. P. Gibbons Jr., G. S. Ibbott, A. J. Mundt, S. Mutic, J. R. Palta, F. Rath, B. R. Thomadsen, J. F. Williamson, and E. D. Yorke. TG-100 Report Part 2: Using Risk Analysis To Design Radiation Therapy Quality Management Programs: IMRT as a Case Study. Medical Physics Report No. (unassigned), To be published 2012b.

JCGM (2008). Joint Committee for Guides in Metrology. JCGM 100:2008 (GUM 1995 with minor corrections). Guide to the Expression of Uncertainty in Measurements (GUM). Sèvres Cedex, France: Bureau International de Poids et Mesures (BIPM), 1993. Subsequently updated in 2010.

Kissick, M. W., J. Fenwick, J. A. James, R. Jeraj, J. M. Kapatoes, H. Keller, T. R. Mackie, G. Olivera, and E. T. Soisson. (2005). "The helical tomotherapy thread effect." *Med Phys* 32(5): 1414–1423.

Klein, E. E., J. Hanley, J. Bayouth, F. F. Yin, W. Simon, S. Dresser, C. Serago, F. Aguirre, L. Ma, B. Arjomandy, C. Liu, C. Sandin, and T. Holmes, (2009). "Task Group 142 report: Quality assurance of medical accelerators." *Med Phys* 36(9): 4197–4212. http://www.aapm.org/pubs/reports/RPT_142.pdf.

Kutcher, G. J., L. Coia, M. Gillin, W. F. Hanson, S. Leibel, R. J. Morton, J. R. Palta, J. A. Purdy, L. E. Reinstein, G. K. Svensson, M. Weller, and L. Wingfield. (1994). "Comprehensive QA for radiation oncology: report of AAPM Radiation Therapy Committee Task Group 40." *Med Phys* 21(4): 581–618. Also available as AAPM Report No. 46. http://www.aapm.org/pubs/reports/rpt_46.pdf.

Lam, K. L., M. S. Muthuswamy, and R. K. Ten Haken. (1998). "Measurement of backscatter to the monitor chamber of medical accelerators using target charge." *Med Phys* 25(3): 334–338.

Langen, K. M., N. Papanikolaou, J. Balog, R. Crilly, D. Followill, S. M. Goddu, W. Grant III, G. Olivera, C. R. Ramsey, and C. Shi. (2010). "QA for helical tomotherapy: Report of the AAPM Task Group 148." *Med Phys* 37(9):4817–4853. http://www.aapm.org/pubs/reports/rpt_148.pdf.

Li, H., A. Lee, X. Zhu, and R. Kudchadker. (2009). "The Effect of Treatment Couch Attenuation On Radiation Dose for Megavoltage Photon Beams." *Med Phys* 36:1. [Abstract SU-FF-T-258]. 51st AAPM Annual Meeting, Anaheim, CA, July 26–30, 2009.

Ling, C. C., P. Zhang, Y. Archambault, J. Bocanek, G. Tang, and T. Losasso. (2008). "Commissioning and quality assurance of RapidArc radiotherapy delivery system." *Int J Radiat Oncol Biol Phys* 72(2):575–581.

Litzenberg, D. W., J. M. Moran, and B. A. Fraass. (2002). "Incorporation of realistic delivery limitations into dynamic MLC treatment delivery." *Med Phys* 29(5):810–820.

Liu, H. H., T. R. Mackie, and E. C. McCullough. (2000). "Modeling photon output caused by backscattered radiation into the monitor chamber from collimator jaws using a Monte Carlo technique." *Med Phys* 27(4):737–744.

LoSasso, T. "Acceptance Testing and Commissioning of IMRT" In: *A Practical Guide to Intensity-Modulated Radiation Therapy*. Memorial Sloan-Kettering staff (eds.). Madison, WI: Medical Physics Publishing, pp. 123–146, 2003.

LoSasso, T., C. S. Chui, and C. C. Ling. (1998). "Physical and dosimetric aspects of a multileaf collimation system used in the dynamic mode for implementing intensity modulated radiotherapy." *Med Phys* 25(10):1919–1927.

Low, D. A., J. M. Moran, J. F. Dempsey, L. Dong, and M. Oldham. (2011). "Dosimetry tools and techniques for IMRT." *Med Phys* 38:1313–1338.

Mahan, S. L., D. J. Chase, and C. R. Ramsey, (2004). "Technical note: Output and energy fluctuations of the TomoTherapy Hi-Art helical tomotherapy system." *Med Phys* 31(7):2119–2120.

Marguet, M., R. Garcia, and M. C. Bordage. (2010). "Evaluation of a new table, Exact IGRT(Varian), on the treatment beam attenuation and the image quality." *Cancer Radiother* 14(1):42–49. [French].

McCormack, S., J. Diffey, and A. Morgan. (2005). "The effect of gantry angle on megavoltage photon beam attenuation by a carbon fiber couch insert." *Med Phys* 32(2):483–487.

Mihaylov, I. B., P. Corry, Y. Yan, V. Ratanatharathorn, and E. G. Moros. (2008). "Modeling of carbon fiber couch attenuation properties with a commercial treatment planning system." *Med Phys* 35(11):4982–4988.

Mitch, M. J., L. A. DeWerd, R. Minniti, and J. F. Williamson. "Treatment of Uncertainties in Radiation Dosimetry" In: *Clinical Dosimetry Measurements in Radiotherapy*. D. W. O. Rogers and J. E. Cygler (eds.). AAPM Medical Physics Monograph No. 34. Proceedings of the 2009 AAPM Summer School, Colorado Springs, CO, June 21–25, 2009. Madison, WI: Medical Physics Publishing, pp. 723–757, 2009.

Moyers, M. F., G. B. Coutrakon, A. Ghebremedhin, K. Shahnazi, P. Koss, and E. Sanders. (2007). "Calibration of a proton beam energy monitor." *Med Phys* 34(6):1952–1966.

Munjal, R. K., P. S. Negi, A. G. Babu, S. N. Sinha, A. K. Anand, and T. Kataria. (2006). "Impact of 6MV photon beam attenuation by carbon fiber couch and immobilization devices in IMRT planning and dose delivery." *J Med Phys* 31(2):67–71.

Myint, W. K., M. Niedbala, D. Wilkins, and L. H. Gerig. (2006). "Investigating treatment dose error due to beam attenuation by a carbon fiber tabletop." *J Appl Clin Med Phys* 7(3):21–27.

Njeh, C. F., T. W. Raines, and M. W. Saunders. (2009). "Determination of the photon beam attenuation by the Brainlab imaging couch: angular and field size dependence." *J Appl Clin Med Phys* 10(3):2979.

Palta, J. R., S. Kim, J. G. Li, and C. Liu. "Tolerance Limits And Action Levels For Planning And Delivery Of IMRT" In: *Intensity-Modulated Radiation Therapy: The State of the Art*. J. R. Palta and T. R. Mackie (eds.). AAPM Medical Physics Monograph No. 29. Proceedings of the 2003 AAPM Summer School, Colorado Springs, CO, June 22–26, 2003. Madison, WI: Medical Physics Publishing, pp. 593–611, 2003.

Pawlicki, T., M. Whitaker, and A. L. Boyer. (2005). "Statistical process control for radiotherapy quality assurance." *Med Phys* 32(9):2777–2786.

Poppe, B., N. Chofor, A. Ruhmann, W. Kunth, A. Djouguela, R. Kollhoff, and K. C. Willborn. (2007). "The effect of a carbon-fiber couch on the depth-dose curves and transmission properties for megavoltage photon beams." *Strahlenther Onkol* 183(1):43–48.

Ramsey, C., R. Seibert, S. L. Mahan, D. Desai, and D. Chase. (2006). "Out-of-field dosimetry measurements for a helical tomotherapy system." *J Appl Clin Med Phys* 7(3):1–11.

Rogers, D. W., B. A. Faddegon, G. X. Ding, C. M. Ma, J. We, and T. R. Mackie. (1995). "BEAM: A Monte Carlo code to simulate radiotherapy treatment units." *Med Phys* 22(5):503–524.

Rosenthal, D. I., J. McDonough, and A. Kassaee. (1998). "The effect of independent collimator misalignment on the dosimetry of abutted half-beam blocked fields for the treatment of head and neck cancer." *Radiother Oncol* 49(3):273–278.

Saw, C. B., and D. H. Hussey. (2000). "Dosimetric assessment of nonperfectly abutted fields using asymmetric collimators." *Med Dosim* 25(1):23–26.

Sawant, A., S. Dieterich, M. Svatos, and P. Keall. (2010). "Failure mode and effect analysis-based quality assurance for dynamic MLC tracking systems." *Med Phys* 37(12): 6466–6479.

Sawkey, D. L. and B. A. Faddegon. (2009a). "Determination of electron energy, spectral width, and beam divergence at the exit window for clinical megavoltage x-ray beams." *Med Phys* 36(3):698–707.

Sawkey, D., and B. A. Faddegon. (2009b). "Simulation of large x-ray fields using independently measured source and geometry details." *Med Phys* 36(12):5622–5632.

Sharpe, M. B., B. M. Miller, D. Yan, and J. W. Wong. (2000). "Monitor unit settings for intensity modulated beams delivered using a step-and-shoot approach." *Med Phys* 27(12):2719–2725.

Sheikh-Bagheri, D., and D. W. O. Rogers. (2002). "Sensitivity of megavoltage photon beam Monte Carlo simulations to electron beam and other parameters." *Med Phys* 29(3): 379–390.

Smith, D. W., D. Christophides, C. Dean, M. Naisbit, J. Mason, and A. Morgan. (2010). "Dosimetric characterization of the iBEAM evo carbon fiber couch for radiotherapy." *Med Phys* 37(7):3595–3606.

Sonke, J. J., B. Brand, and M. van Herk. (2003). "Focal spot motion of linear accelerators and its effect on portal image analysis." *Med Phys* 30(6):1067–1075.

Spezi, E., and A. Ferri. (2007). "Dosimetric characteristics of the Siemens IGRT carbon fiber tabletop." *Med Dosim* 32(4):295–298.

Thomas, S. D., M. Mackenzie, G. C. Field, A. M. Syme, and B. G. Fallone. (2005). "Patient specific treatment verifications for helical tomotherapy treatment plans." *Med Phys* 32(12):3793–3800.

Van Esch, A., C. Clermont, M. Devillers, M. Iori, and D. P. Huyskens. (2007). "On-line quality assurance of rotational radiotherapy treatment delivery by means of a 2D ion chamber array and the Octavius phantom." *Med Phys* 34(10):3825–3837.

Van Prooijen, M., T. Kanesalingam, M. K. Islam, and R. K. Heaton. (2010). "Assessment and management of radiotherapy beam intersections with the treatment couch." *J Appl Clin Med Phys* 11(2):3171.

Verhaegen, F., R. Symonds-Tayler, H. H. Liu, and A. E. Nahum. (2000). "Backscatter towards the monitor ion chamber in high-energy photon and electron beams: Charge integration versus Monte Carlo simulation." *Phys Med Biol* 45(11):3159–3170.

Vieira, S. C., R. S. Kaatee, M. L. Dirkx, and B. J. Heijmen. (2003). "Two-dimensional measurement of photon beam attenuation by the treatment couch and immobilization devices using an electronic portal imaging device." *Med Phys* 30(11):2981–2987.

Weber, L., P. Nilsson, and A. Ahnesjö (1997). "Build-up cap materials for measurement of photon head-scatter factors." *Phys Med Biol* 42(10):1875–1886.

Westerly, D. C., E. Soisson, Q. Chen, K. Woch, L. Schubert, G. Olivera, and T. R. Mackie. (2009). "Treatment planning to improve delivery accuracy and patient throughput in helical tomotherapy." *Int J Radiat Oncol Biol Phys* 74(4):1290–1297.

Zhu, T. C., A. Ahnesjö, K. L. Lam, X. A. Li, C. M. Ma, J. R. Palta, M. B. Sharpe, B. Thomadsen, and R. C. Tailor. (2009). "Report of AAPM Therapy Physics Committee Task Group 74: In-air output ratio, S_c, for megavoltage photon beams." *Med Phys* 36(11): 5261–5291. http://www.aapm.org/pubs/reports/RPT_97.pdf,